

Holographic Superconductors

En-Jui Chang,^{1,*} Chia-Jui Chou,^{1,†} and Yi Yang^{1,‡}

¹*Department of Electrophysics, National Chiao Tung University, Hsinchu, ROC*

Abstract

We study a non-minimal holographic superconductors model in both non-backreaction and full-backreaction cases using an analytic method. We calculate the condensate of the dilaton and the critical temperature of the phase transition. We also study the properties of the electric conductivity in various parameters.

arXiv:1812.04288v2 [hep-th] 27 Dec 2018

*Electronic address: phyenjui@gmail.com

†Electronic address: agoodmanjerry.ep02g@nctu.edu.tw

‡Electronic address: yyang@mail.nctu.edu.tw

Contents	
I. Introduction	2
II. Einstein-Maxwell-Scalar System	3
III. Non-Backreaction	8
IV. Full-Backreaction	12
A. Matching Solutions	13
B. Condensate	15
C. Conductivity	17
V. Conclusion	22
Acknowledgements	23
Appendices	23
A. Condensate near critical temperature	23
B. Formulas with full-backreaction	24
References	26

I. INTRODUCTION

The perturbation technique is a standard approach in the conventional quantum field theories. However, it only works for the weakly coupled systems. It is well known that the traditional BCS theory [1] which describes the weakly coupled electron-phonon interaction is very successful. However, the high critical temperature T_c superconductivity involves the strong couplings beyond the BCS theory.

The AdS/CFT duality [2–6] is a powerful tool to study a d -dimensional strongly coupled conformal field theories (CFT) by studying its $d + 1$ -dimensional dual gravitational theory in an Anti de Sitter (AdS) space, and vice versa. It is interesting to study the strongly coupled superconductivity via the AdS/CFT duality, and this kind of the superconductors

models are called the holographic superconductors (HSC) [7–13].

In the last decade, the HSC has been studied in both the non-backreaction case [8, 11, 14–45] and the backreaction case [9, 12, 46–60]. Most of these studies are based on the numerical methods [45, 47–51, 54, 61–75], while some others used the analytic methods [52, 53, 55, 57, 58, 76–87]. In [77–87], an approximate analytic method, matching method, has been developed to study the holographic correspondence in the non-backreaction case.

In this work, we will study a non-minimal holographic superconductor model with two parameters using the matching method in both the non-backreaction and the full-backreaction cases. By solving the system analytically, we study the condensate of the dilaton which acts as a order parameter of a second order phase transition. The critical temperatures of phase transition are calculated. We find that the condensate of dilaton in the non-backreaction case is not consistent with numeric results, but the one in the full-backreaction case produces the correct results. In addition, we study the electric conductivity using an analytic truncating method.

This paper is organized as follow: In section II, we introduce the EMD system and describe the matching method to solve the system. In section III, we study the condensate of dilaton in the non-backreaction case. In section IV, we study both the condensate and the electric conductivity in the full backreaction case . We summarize our results in section V.

II. EINSTEIN-MAXWELL-SCALAR SYSTEM

In this paper, we consider a 4-dimensional Einstein-Maxwell-Scalar (EMS) system, which includes a gravity field $g_{\mu\nu}$, a Maxwell field A_μ and a charged complex scalar field $\Phi = \phi e^{i\theta}$. After fixing the Stückelberg field $\theta = 0$, the action can be expressed as,

$$S = \frac{1}{16\pi G_4} \int dz d^3x \sqrt{-g} \left[R - \frac{f(\phi)}{4} F^{\mu\nu} F_{\mu\nu} + \frac{6}{\ell^2} U(\phi) - \frac{1}{2} (\partial^\mu \phi \partial_\mu \phi) - \frac{J(\phi)}{2} A^\mu A_\mu \right], \quad (2.1)$$

where $f(\phi)$ is the gauge kinetic function which describes the interaction between the gauge field and the scalar field, $U(\phi)$ is the scalar potential and $J(\phi)$ is the extended Stückelberg

function that preserve the gauge invariant. In this paper, we choose

$$f(\phi) = 1 + \frac{\alpha^2}{2}\phi^2, \quad (2.2a)$$

$$U(\phi) = 1 - \frac{\ell^2}{12}m^2\phi^2, \quad (2.2b)$$

$$J(\phi) = q^2\phi^2. \quad (2.2c)$$

The similar system has been studied numerically in [48]. There are four free parameters (α, q, m, ℓ) in the action. We will analytically study the system by using the matching method and compare our results with the ones in the numerical method.

The equations of motion are obtained by varying the action with the different fields,

$$R_{\mu\nu} - \frac{1}{2}g_{\mu\nu} \left[R - \frac{f(\phi)}{4}F^{\rho\sigma}F_{\rho\sigma} + \frac{6}{\ell^2}U(\phi) - \frac{1}{2}(\partial^\rho\phi\partial_\rho\phi) - \frac{J(\phi)}{2}A^\rho A_\rho \right] - \frac{f(\phi)}{2}F_{\mu\rho}F_\nu{}^\rho - \frac{1}{2}\partial_\mu\phi\partial_\nu\phi - \frac{J(\phi)}{2}A_\mu A_\nu = 0, \quad (2.3a)$$

$$\nabla_\mu [f(\phi)F^{\mu\nu}] - J(\phi)A^\nu = 0, \quad (2.3b)$$

$$\nabla^2\phi - \frac{1}{4}\frac{\partial f(\phi)}{\partial\phi}F^{\mu\nu}F_{\mu\nu} + \frac{6}{\ell^2}\frac{\partial U(\phi)}{\partial\phi} - \frac{1}{2}\frac{\partial J(\phi)}{\partial\phi}A^\mu A_\mu = 0. \quad (2.3c)$$

Since we are going to study the thermodynamic properties in the HSC system at the finite temperature, we consider a black hole background that asymptotic to the AdS space. Without loss of generality, we consider the following ansatz of an isotropic black hole,

$$ds^2 = -g(r)e^{-\chi(r)}dt^2 + \frac{dr^2}{g(r)} + r^2(dx^2 + dy^2), \quad (2.4a)$$

$$A = A_t(r)dt, \quad (2.4b)$$

$$\phi = \phi(r), \quad (2.4c)$$

where r is the holographic radius which corresponds to the energy scale in the dual field theory. The Hawking temperature of the black hole can be calculated as,

$$T = \frac{1}{4\pi}g(r)'e^{-\frac{\chi(r)}{2}} \Big|_{r=r_H}, \quad (2.5)$$

where the black hole horizon r_H is defined by $g(r_H) = 0$.

Plugging the ansatz (2.4) into the equations of motion (2.3) leads to the following equa-

tions of motion for the background fields:

$$\chi' + \frac{r}{2}\phi'^2 + \frac{rJ}{2g^2}e^{\chi}A_t^2 = 0, \quad (2.6a)$$

$$\frac{g'}{rg} + \frac{1}{r^2} + \frac{1}{4}\phi'^2 - \frac{3}{\ell^2g}U(\phi) + \frac{f}{4g}e^{\chi}A_t^2 + \frac{J}{4g^2}e^{\chi}A_t^2 = 0, \quad (2.6b)$$

$$A_t'' + \left(\frac{f'}{f} + \frac{2}{r} + \frac{\chi'}{2}\right)A_t' - \frac{J}{gf}A_t = 0, \quad (2.6c)$$

$$\phi'' + \left(\frac{g'}{g} + \frac{2}{r} - \frac{\chi'}{2}\right)\phi' + \left(\frac{6U'}{\ell^2g} + \frac{e^{\chi}A_t^2Jf'}{2g} + \frac{e^{\chi}A_t^2J'}{2g^2}\right)\frac{1}{\phi'} = 0, \quad (2.6d)$$

where the prime represents the derivative with respect to r .

It is easy to verify that the RN-AdS black hole is a simple solution of the above equations of motion (2.6),

$$g(r) = \frac{r^2}{\ell^2} - \frac{1}{r} \left(\frac{r_H^3}{\ell^2} + \frac{\rho^2}{4r_H} \right) + \frac{\rho^2}{4r^2}, \quad (2.7a)$$

$$A_t = \rho \left(\frac{1}{r_H} - \frac{1}{r} \right), \quad (2.7b)$$

$$\chi(r) = \phi(r) = 0. \quad (2.7c)$$

In the following, we will find an approximate analytic solution of the equations of motion (2.6) by the matching method. (If we have the exact solution, we can get the series expansion to all orders at any point in principle. These series expansion are identical at any points. Obviously, there is no closed form to the solutions of the equations of motion (2.6).) Instead of solving the equations of motion (2.6) exactly, we solve for the background fields near the horizon at $r = r_H$ and near the boundary at $r = \infty$, respectively. Given the boundary conditions at either the horizon or the boundary, the background fields can be determined order by order. We then match the two solutions near the horizon and the boundary at some intermediate points $r_m \in (r_H, \infty)$ by requiring the continuous or even the smooth conditions for the background fields. Obviously, the solutions by matching are only the good approximation at the horizon and the boundary, but not the exact solutions of the equations of motion for every r . Nevertheless, since the core of the holographic correspondence is to relate the field theory on the boundary and the near horizon geometry of the bulk, we believe that the detail behavior of the solution at the intermediate part does not affect the physics too much. We thus can trust the physics from the results of this approximate matching solution at least qualitatively.

It is convenient to make a coordinate transformation from r to $z = r_H/r \in (0, 1)$ with the boundary at $z = 0$ and the black hole horizon at $z = 1$. In this work, to be concrete, we choose the matching point as $z_m = 3/4$. With the new coordinate z , the equations of motion for the background fields become,

$$\chi' - \frac{z}{2}\phi'^2 - \frac{r_H^2 B^2}{2z^3 g^2} = 0, \quad (2.8a)$$

$$g' - \left(\frac{1}{z} + \frac{\chi'}{2}\right)g - \frac{zf}{4}\left(B' - \frac{\chi'}{2}B\right)^2 + \frac{3r_H^2}{z^3 \ell^2}U = 0, \quad (2.8b)$$

$$B'' + \left(\frac{f'}{f} - \frac{\chi'}{2}\right)B' - \left(\frac{\chi''}{2} + \frac{\chi' f'}{2f} + \frac{1}{z^4} \frac{r_H^2 J}{gf}\right)B = 0, \quad (2.8c)$$

$$\phi'' + \left(\frac{g'}{g} - \frac{\chi'}{2}\right)\phi' + \left[\frac{\left(B' - \frac{\chi'}{2}B\right)^2 f'}{2g} + \frac{r_H^2 B^2 J'}{2z^4 g^2} + \frac{6r_H^2 U'}{z^4 \ell^2 g}\right] \frac{1}{\phi'} = 0. \quad (2.8d)$$

where the prime represents the derivative with respect to z now, and we have defined a new field $B^2 = e^{\chi} A_t^2$ for convenience.

The series expansions of the background fields near the horizon can be written as:

$$\chi(z) = \sum_{k=0}^{\infty} \chi_k (1-z)^k, \quad (2.9a)$$

$$g(z) = \frac{r_H^2}{\ell^2 z^2} \left[1 - z^3 + \sum_{k=0}^{\infty} g_k (1-z)^k \right], \quad (2.9b)$$

$$B(z) = \sum_{k=0}^{\infty} B_k (1-z)^k, \quad (2.9c)$$

$$\phi(z) = \sum_{k=0}^{\infty} \phi_k (1-z)^k, \quad (2.9d)$$

In the above expansions, because the differential equations for χ and g are first order and the differential equations for B and ϕ are second order, there are six coefficients ($\chi_0, g_0, B_0, B_1, \phi_0, \phi_1$) can be chosen as the boundary conditions at the horizon $z = 1$, while the other higher ordered coefficients can be obtained from these six coefficients by solving the equations of motion order by order.

Specially, the boundary condition to define the horizon $g(1) = 0$ leads $g_0 = 0$. Furthermore, the regularity boundary conditions at the horizon require,

$$B_0 = 0, \quad (2.10a)$$

$$\phi_1 = -\frac{1}{g'} \left(6 \frac{\partial U(\phi)}{\partial \phi} + \frac{B_1^2}{2} \frac{\partial f(\phi)}{\partial \phi} \right) \Big|_{z=1}. \quad (2.10b)$$

In this work, for the least approximation, we only take the expansions at the horizon up to the order $k = 1$ for the fields χ and g , and to the order $k = 2$ for the fields B and ϕ . The series expansion of the background fields near the horizon become,

$$\chi(z) = \chi_0 + \chi_1(1-z), \quad (2.11a)$$

$$g(z) = \frac{r_H^2}{\ell^2 z^2} [1 - z^3 + g_1(1-z)], \quad (2.11b)$$

$$B(z) = B_1(1-z) + B_2(1-z)^2, \quad (2.11c)$$

$$\phi(z) = \phi_0 + \phi_1(1-z) + \phi_2(1-z)^2, \quad (2.11d)$$

where ϕ_1 is given in Eq. (2.10b) and only three coefficients ($\chi_0, B_1, \phi_0,$) left to be given.

At the boundary $z = 0$, the asymptotic behavior of the fields are,

$$\chi(z) \sim \chi^{(0)} + \frac{\Delta_{\pm} D_{\Delta_{\pm}}^2}{4\ell^2 r_H^{2\Delta_{\pm}}} z^{2\Delta_{\pm}}, \quad (2.12a)$$

$$g(z) \sim \begin{cases} \frac{r_H^2}{\ell^2 z^2} - \frac{2M}{r_H} z + \frac{\Delta_{\pm}}{4\ell^2} \frac{D_{\Delta_{\pm}}^2}{r_H^{2\Delta_{\pm}-2}} z^{2\Delta_{\pm}-2} & \frac{1}{2} < \Delta_{\pm} \leq \frac{3}{2}, \\ \frac{r_H^2}{\ell^2 z^2} - \frac{2M}{r_H} z & \frac{3}{2} < \Delta_{\pm}, \end{cases} \quad (2.12b)$$

$$B(z) \sim \mu - \frac{\rho}{r_H} z, \quad (2.12c)$$

$$\phi(z) \sim \frac{D_{\Delta_-}}{r_H^{\Delta_-}} z^{\Delta_-} + \frac{D_{\Delta_+}}{r_H^{\Delta_+}} z^{\Delta_+} \quad (2.12d)$$

where

$$\Delta_{\pm} = \frac{3 \pm \sqrt{9 + 4m^2\ell^2}}{2}. \quad (2.13)$$

are the conformal dimensions for the scalar fields with mass m .

Similarly, in the above asymptotic forms, there are six coefficients ($\chi^{(0)}, M, \mu, \rho, D_{\Delta_-}, D_{\Delta_+}$) can be chosen as the boundary conditions at the boundary $z = 0$. The asymptotic coefficients μ and ρ in $B(z)$ are chemical potential and charge density. The asymptotic coefficients D_{Δ_-} and D_{Δ_+} in $\phi(z)$ represent the condensates.

To satisfy the conformal symmetry, we should fix either $D_{\Delta_-} = 0$ or $D_{\Delta_+} = 0$ to obtain a stable solution. Both boundary conditions are allowed and we choose $D_{\Delta_-} = 0$ for convention in this work. Setting $m^2\ell^2 = -2$, we have $\Delta_- = 1$ and $\Delta_+ = 2$. With our choices, the

asymptotic behavior of the background fields at the boundary $z = 0$ becomes,

$$\chi(z)x \sim \chi^{(0)} + \frac{1}{2\ell^2} \frac{D_2^2}{r_H^4} z^4, \quad (2.14a)$$

$$g(z) \sim \frac{r_H^2}{\ell^2 z^2} - \frac{2M}{r_H} z, \quad (2.14b)$$

$$B(z) \sim \mu - \frac{\rho}{r_H} z, \quad (2.14c)$$

$$\phi(z) \sim \frac{D_2}{r_H^2} z^2, \quad (2.14d)$$

where only five coefficients ($\chi^{(0)}, M, \mu, \rho, D_2$) left to be given.

III. NON-BACKREACTION

We first consider the case of non-backreaction, i.e. we treat the field ϕ and B as the probe fields which do not affect the spacetime background. By setting $\phi = B = 0$, the equations of motion (2.8) for the background fields reduces to

$$\chi' = 0, \quad (3.1a)$$

$$g' - \frac{g}{z} + \frac{3r_H^2}{z^3 \ell^2} = 0, \quad (3.1b)$$

which admits the simple AdS-Schwarzschild black hole solution,

$$\chi(z) = 0, \quad (3.2a)$$

$$g(z) = \frac{r_H^2}{\ell^2 z^2} (1 - z^3), \quad (3.2b)$$

with the black hole temperature $T = 3r_H^2/l^2$.

Next, we are going to solve the equations of motion for the probe fields B and ϕ ,

$$B'' + \frac{f'(z)}{f} B' - \frac{1}{z^4} \frac{r_H^2 J}{g f} B = 0, \quad (3.3a)$$

$$\phi'' + \frac{g'}{g} \phi' + \left[\frac{B'^2 f'}{2g} + \frac{r_H^2 B^2 J'}{2z^4 g^2} + \frac{6r_H^2 U'}{z^4 \ell^2 g} \right] \frac{1}{\phi'} = 0. \quad (3.3b)$$

There are two scaling symmetries in the equations of motion (3.3) with the form $C \rightarrow s^{-n_C} C$, where C is one of the variables ($r, t, \vec{x}, g, B, \ell, q$), s is a scaling factor and n_C is the scaling dimension for C . The scaling dimensions for the two scaling symmetries are listed in Table I.

Sym.	n_r	n_t	$n_{\vec{x}}$	n_g	n_B	n_ℓ	n_q
I	1	-1	-1	2	1	0	0
II	1	0	1	0	0	1	-1

TABLE I: The two scaling symmetries of the equations of motion (3.3) in the case of non-backreaction.

We can use the above two scaling symmetries to set $\ell = 1$ and $\rho = \text{constant}$.

In the case of non-backreaction, the series expansions of the fields B and ϕ near the horizon in Eqs.(2.11) becomes,

$$B(z) = a(1-z) + B_2(1-z)^2, \quad (3.4a)$$

$$\phi(z) = b + \phi_1(1-z) + \phi_2(1-z)^2, \quad (3.4b)$$

where we have renamed $B_1 = a$ and $\phi_0 = b$ in (2.11). a and b will be imposed as the boundary values at the horizon $z = 1$. Plug the series expansions (3.4) into the equations of motion (3.3), B_2 , ϕ_1 and ϕ_2 can be solved in terms of the boundary values a and b order by order,

$$B_2 = \frac{1}{6} \frac{((4\alpha^2 + 2q^2)r_H^2 + a^2\alpha^4)b^2a}{r_H^2(\alpha^2b^2 + 2)}, \quad (3.5a)$$

$$\phi_1 = -\frac{1}{6} \frac{b(\alpha^2a^2 + 4r_H^2)}{r_H^2} \quad (3.5b)$$

$$\begin{aligned} \phi_2 = & -\frac{1}{48} \frac{b}{r_H^4(\alpha^2b^2 + 2)} \left\{ \left(\frac{32\alpha^2b^2}{3} + \frac{64}{3} \right) r_H^4 \right. \\ & \left. + 4a^2 \left[-\frac{1}{3}\alpha^4b^2 + \left(b^2q^2 - \frac{10}{3} \right) \alpha^2 + \frac{2}{3}q^2 \right] r_H^2 + a^4\alpha^4 \left(\alpha^2b^2 - \frac{2}{3} \right) \right\}. \end{aligned} \quad (3.5c)$$

At the boundary $z = 0$, the asymptotic behavior of the fields B and ϕ are the same as in Eqs. (2.14),

$$B(z) \sim \mu - \frac{\rho}{r_H} z, \quad (3.6a)$$

$$\phi(z) \sim \frac{D_2}{r_H^2} z^2. \quad (3.6b)$$

where μ and D_2 will be imposed as the boundary values at the boundary $z = 0$.

The two boundary values a and b at the horizon $z = 1$ and the two boundary values μ and D_2 at the boundary $z = 0$ are related by the matching conditions of the fields B and ϕ at a matching point z_m .

To match the series expansions of the fields $B(z)$ and $\phi(z)$ at the horizon in Eq. (3.4) and that at the boundary in Eq. (3.6) smoothly at a matching point z_m , we require the following four constraint equations,

$$\mu - \frac{\rho}{r_H} z_m = a(1 - z_B) + B_2(1 - z_m)^2, \quad (3.7a)$$

$$-\frac{\rho}{r_H} = -a - 2B_2(1 - z_B), \quad (3.7b)$$

$$\frac{D_2}{r_H^2} z_m^2 = b + \phi_1(1 - z_m) + \phi_2(1 - z_m)^2, \quad (3.7c)$$

$$\frac{2D_2}{r_H^2} z_m = -\phi_1 - 2\phi_2(1 - z_m). \quad (3.7d)$$

The above constraint equations can be solved as,

$$\mu = a + B_2(1 - z_m)(1 + z_m), \quad (3.8a)$$

$$\rho = [a + 2B_2(1 - z_m)]r_H, \quad (3.8b)$$

$$D_2 = \frac{b}{12z_m} [12r_H^2 - (\alpha^2 a^2 + 4r_H^2)(1 - z_m)], \quad (3.8c)$$

$$0 = 2b + \phi_1(2 - z_m) + 2\phi_2(1 - z_m), \quad (3.8d)$$

To be concrete, we take $z_m = 3/4$ in the following calculation. The two parameters a and b can be analytically solved from Eqs. (3.8b) and (3.8d) once the charge density ρ is given,

$$b^2 = \frac{-24r_H(ar_H - \rho)}{2a(8\alpha^2 + q^2)r_H^2 - 12\alpha^2 r_H \rho + \alpha^4 a^3}, \quad (3.9)$$

with a satisfies a quartic equation,

$$\alpha^4 a^4 - 4r_H^2(-2\alpha^2 + q^2)a^2 - 48r_H \rho \alpha^2 a + 304r_H^4 = 0. \quad (3.10)$$

The condensate D_2 is the order parameter of the superconducting phase transition. Above a critical temperature T_c , the order parameter $D_2 \propto b$ is zero, which from Eq. (3.9) implies $ar_H - \rho = 0$ at the critical temperature T_c . From Eq. (3.10), we obtain the critical temperature by taking $a = \rho/r_H$,

$$T_c = \frac{3}{4\pi} \left(\frac{10\alpha^2 + q^2 + \sqrt{24\alpha^4 + 20\alpha^2 q^2 + q^4}}{152} \right)^{1/4} \rho^{1/2}. \quad (3.11)$$

For $\alpha = q = 0$, T_c vanishes, there is no phase transition at this special point. For $\alpha \gg q$, the critical temperature $T_c \propto \alpha^{1/2}$; While for $\alpha \ll q$, the critical temperature $T_c \propto q^{1/2}$.

The critical temperature T_c is proportional to $\sqrt{\rho}$ and increases with α and q monotonously. $T_c/\sqrt{\rho}$ vs. the parameters (α, q) is plotted in Fig. 1. The behavior of the analytic expression of the critical temperature in Eq. (3.11) is consistent with the numeric result in [48].

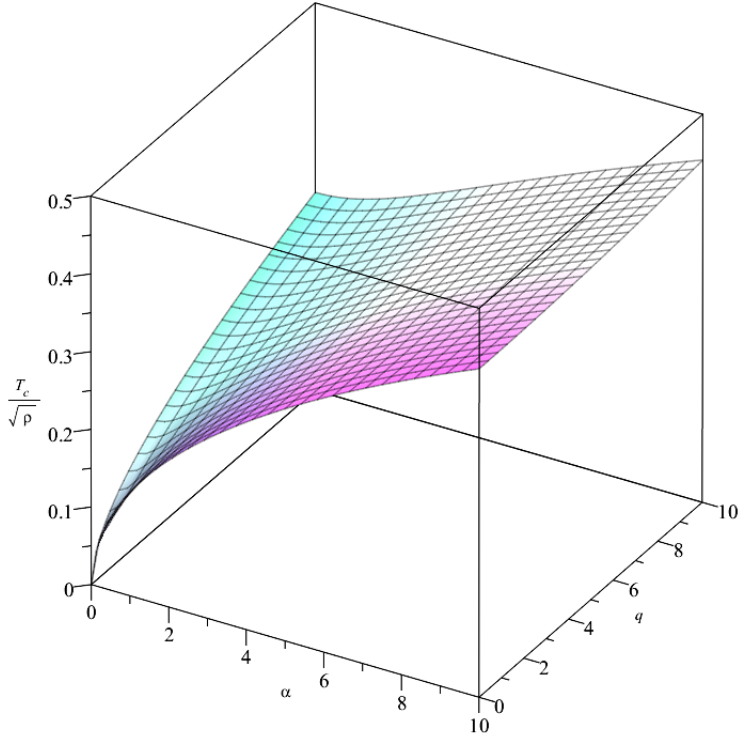


FIG. 1: $T_c/\sqrt{\rho}$ varies with the couplings α, q .

Near the critical temperature T_c , the condensate behaves as $D_2 = AT_c^2(1 - T/T_c)^{1/2}$, which indicates that the phase transition at T_c is a second order phase transition. The coefficient A depends on the parameters α, q and ρ , see Eq. (A.1) in the Appendix.

The condensate D_2 vs. T/T_c for $\alpha = q = 1$ can be calculated from Eq. (3.8c) and is plotted as the solid line in Fig. 2. We see that the low temperature behavior of condensate in the non-backreaction calculation (red line) is not consistent with the numeric calculation in [48]. The blue line in Fig. 2 is the condensate near the critical temperature and is exploited to the low temperature region.

The inconsistency of the condensate around the low temperature is due to the non-backreaction approximation we took in this section. In the next section, we will study the full backreaction case.

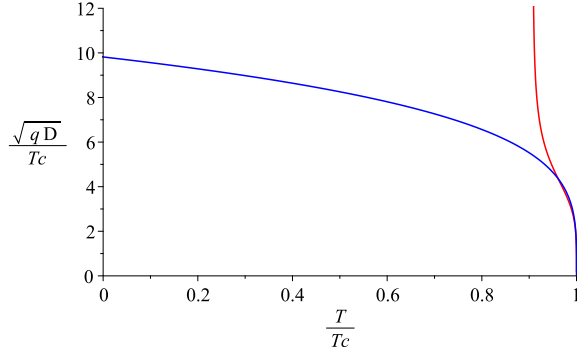


FIG. 2: The behavior of the condensate D_2 with the couplings $\alpha = 1$, $q = 1$. The red line is the condensate directly from Eq. (3.8c), while the blue line is the approximate condensate near the critical temperature T_c .

IV. FULL-BACKREACTION

In this section, we consider the case of full-backreaction by including the backreacted effects of the fields B and ϕ . It is necessary to solve the fields χ and g in the metric (2.4a) as well as the fields B and ϕ together from the full equations of motion (2.8).

Similarly to the non-backreaction case, there are three scaling symmetries in the equations of motion (2.8) in the full-backreaction case. The scaling dimensions of these variables for the scaling symmetries are listed in Table II.

Sym.	n_r	n_t	$n_{\vec{x}}$	n_{r_H}	$n_{e\chi}$	n_g	n_B	n_ℓ	n_q
I	1	1	0	0	2	0	0	0	0
II	1	-1	-1	1	0	2	1	0	0
III	1	1	0	1	0	0	0	1	-1

TABLE II: Scaling symmetries in the equations of motion (2.8) with full-backreaction.

As in the non-backreaction case, we can use the three scaling symmetries to set the parameters $\ell = 1$, $\rho = \text{constant}$ and $\chi^{(0)} = 0$ in Eq. (2.12a), which are the necessary boundary conditions to ensure the asymptotic AdS at the boundary.

A. Matching Solutions

Similarly as what we have done in the non-backreaction case, we will solve the fields (χ, g, B, ϕ) in the full-backreaction case by using the matching method.

Up to the order next to the initial values, the series expansions of the fields (χ, g, B, ϕ) near horizon in (2.11) becomes,

$$\chi(z) = \chi_0 + \chi_1(1-z), \quad (4.1a)$$

$$g(z) = \frac{r_H^2}{z^2} [1 - z^3 + g_1(1-z)], \quad (4.1b)$$

$$B(z) = a(1-z) + B_2(1-z)^2, \quad (4.1c)$$

$$\phi(z) = b + \phi_1(1-z) + \phi_2(1-z)^2, \quad (4.1d)$$

where we have renamed $B_1 = a$ and $\phi_0 = b$ in (2.11). In the above expansion, χ_0 , a and b need to be imposed as the boundary values at the horizon $z = 1$. Plug the series expansions (4.1) into the equations of motion (2.8), we can solve for the coefficients $(\chi_1, g_1, B_2, \phi_2)$ in Eqs. (4.1) in terms of the boundary values (χ_0, a, b) .

$$g_1 = \frac{1}{8r_H^2} (4b^2r_H^2 - a^2(\alpha^2b^2 + 2)), \quad (4.2a)$$

$$\phi_1 = -\frac{(a^2\alpha^2 + 4r_H^2)b}{2(g_1 + 3)r_H^2}, \quad (4.2b)$$

$$\chi_1 = \frac{-\phi_1^2(g_1 + 3)^2r_H^2 - a^2}{2(g_1 + 3)^2r_H^2}, \quad (4.2c)$$

$$B_2 = \frac{a((1/4\chi_1(g_1 + 3)\alpha^2 + q^2)b^2 - \phi_1\alpha^2(g_1 + 3)b + 1/2(g_1 + 3)\chi_1)}{(\alpha^2b^2 + 2)(g_1 + 3)}, \quad (4.2d)$$

$$\begin{aligned} \phi_2 = & \frac{1}{8(g_1 + 3)^2r_H^2} [((((\chi_1 + 4)b - \phi_1)g_1 + (3\chi_1 + 15)b - 3\phi_1)\alpha^2 - 2bq^2)a^2 - 4bB_2\alpha^2(g_1 + 3)a \\ & + 12r_H^2(1/12g_1^2\chi_1\phi_1 + 1/2(\chi_1 + 7/3)\phi_1g_1 + b + \phi_1(3/4\chi_1 + 7/2))]. \end{aligned} \quad (4.2e)$$

The detailed forms are listed in (B.2).

At the boundary $z = 0$, the asymptotic behavior of the fields (χ, g, B, ϕ) was listed in Eq. (2.14), where M , μ and D_2 will be imposed as the boundary values at the boundary $z = 0$.

The three boundary values (χ_0, a, b) at the horizon $z = 1$ and the three boundary values (M, μ, D_2) at the boundary $z = 0$ are related by six matching conditions of the fields (χ, g, B, ϕ) at a matching point z_m .

To match the asymptotic behaviors of the fields at the horizon in Eq. (2.14) and that at the boundary in Eq. (4.1) smoothly at a matching point z_m , we require the following six constraint equations,

$$\frac{1}{2} \left(\frac{D_2}{r_H^2} z_m^2 \right)^2 = \chi_0 + \chi_1 (1 - z_m), \quad (4.3a)$$

$$\frac{1 - 2M z_m^3 r_H^2}{z_m^2} = \frac{1 - z_m^3 r_H^2}{z_m^2} + g_1 \frac{(1 - z_m)}{z_m^2} r_H^2, \quad (4.3b)$$

$$\mu - \frac{\rho}{r_H} z_m = a (1 - z_m) + B_2 (1 - z_m)^2, \quad (4.3c)$$

$$-\frac{\rho}{r_H} = -a - 2B_2 (1 - z_m), \quad (4.3d)$$

$$\frac{D_2}{r_H^2} z_m^2 = b + \phi_1 (1 - z_m) + \phi_2 (1 - z_m)^2, \quad (4.3e)$$

$$2 \frac{D_2}{r_H^2} z_m = -\phi_1 - 2\phi_2 (1 - z_m), \quad (4.3f)$$

which can be solved as

$$\chi_0 = -\chi_1 (1 - z_m) + \frac{1}{2} \left(\frac{D_2}{r_H^2} \right)^2 z_m^4, \quad (4.4a)$$

$$M = \frac{1}{2} - \frac{g_1 (1 - z_m)}{2z_m^3}, \quad (4.4b)$$

$$\mu = a + B_2 (1 - z_m) (1 + z_m), \quad (4.4c)$$

$$\rho = \left[a + 2B_2 (1 - z_m) \right] r_H, \quad (4.4d)$$

$$D_2 = \frac{2b + \phi_1 (1 - z_m)}{2z_m} r_H^2, \quad (4.4e)$$

$$0 = 2b + \phi_1 (2 - z_m) + 2\phi_2 (1 - z_m). \quad (4.4f)$$

The same as in the non-backreaction case, we take $z_m = 3/4$ in the following. Eq.(4.4f) can be expressed as a cubic equation of a^2 , see Eq. (B.6), which can be solved analytically in term of b^2 .

We check the stability of the analytic hairy black hole solution by comparing its free energies with the free energies of RN black holes are obtained in Eqs. (2.7),

$$F_{\text{Hairy}} = V (-2M + \mu\rho), \quad (4.5a)$$

$$F_{\text{RN}} = \frac{V}{r_H} \left(-r_H^4 + \frac{3\rho^2}{4} \right). \quad (4.5b)$$

For the given couplings α and q , as well as a charge density ρ , the free energies F_{Hairy} and F_{RN} vs. T/T_c are plotted in Fig. 3.

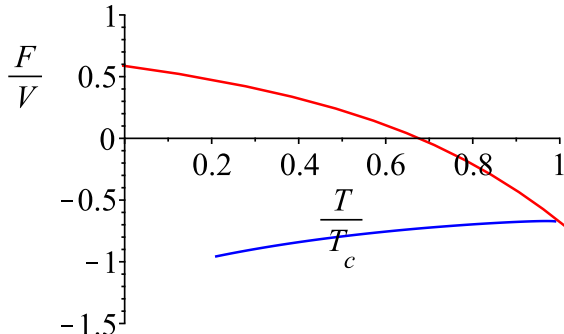


FIG. 3: The free energies $\frac{F_{Hairy}}{V}$ (blue) and $\frac{F_{RN}}{V}$ (red) with $\alpha = 5$, $q = 1$, and $\rho = \text{constant}$ for $T \leq T_c$.

When $T < T_c$, the free energy of the hairy black hole is always lower than that of the RN black hole and vice versa. Thus for $T > T_c$, the system is in the RN black hole phase with the scalar field $\phi = 0$; while for $T < T_c$, the system transits to the hairy black hole phase with $\phi \neq 0$ that indicates the condensation.

B. Condensate

In this section, we investigate the condensate D_2 , the order parameter of the superconducting phase transition, in more details. The behavior of the order parameter $D_2 \propto b$ around the critical temperature is the same as that in the non-backreaction case, $D_2 \propto (1 - T/T_c)^{1/2}$. However, the fixed- ρ condition has been modified at the critical temperature ($B_2|_{T=T_c} \neq 0$). The condensate D_2 vs the ratio of the temperature T/T_c for different parameters α and q are plotted in Fig. 4 and 5.

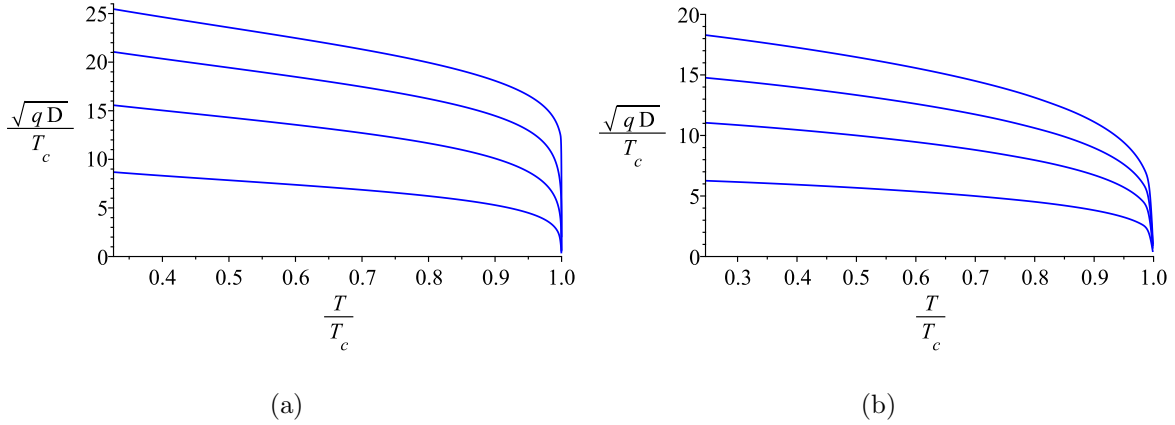


FIG. 4: The condensate to temperature diagram with the coupling $q = 1, 3, 5, 7$ from bottom to top and (a) $\alpha = 1$, (b) $\alpha = 5$.

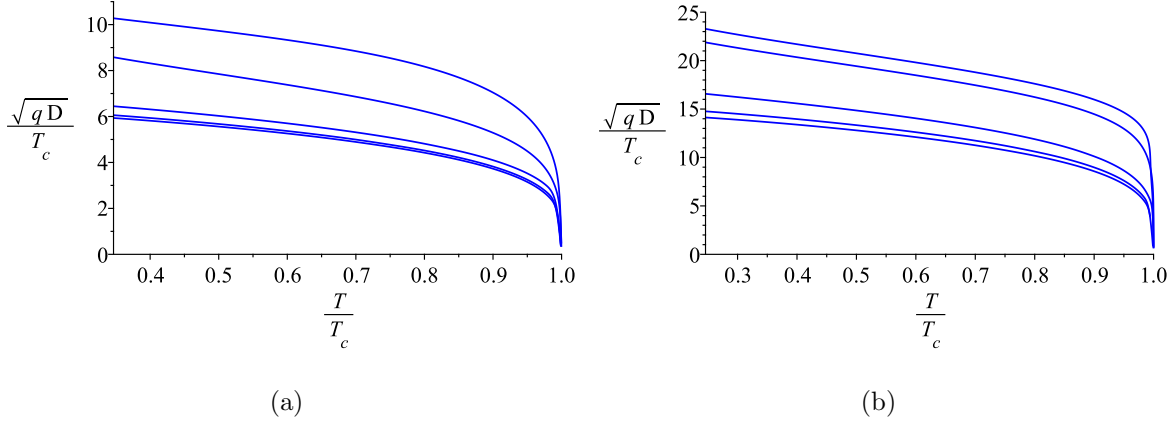


FIG. 5: The condensate to temperature diagram with the coupling $\alpha = 10^{-4}, 1, 3, 5, 7$ from top to bottom and (a) $q = 1$, (b) $q = 5$.

From Fig. 4 and Fig. condensate alpha, we see that, for a fixed α , the condensate D_2 increases as the parameter q increases, while for a fixed q , the condensate D_2 decreases as the parameter α increases. The behavior of the condensate D_2 depending on the parameters α and q is consistent with the numeric result in [48].

As we did in the non-backreaction case, the critical temperature in the full-backreaction case can be obtained analytically, but the expression is much more complicated. The behavior of the critical temperature T_c in the full-backreaction case is also similar to that in the non-backreaction case and is plotted in Fig. 6.

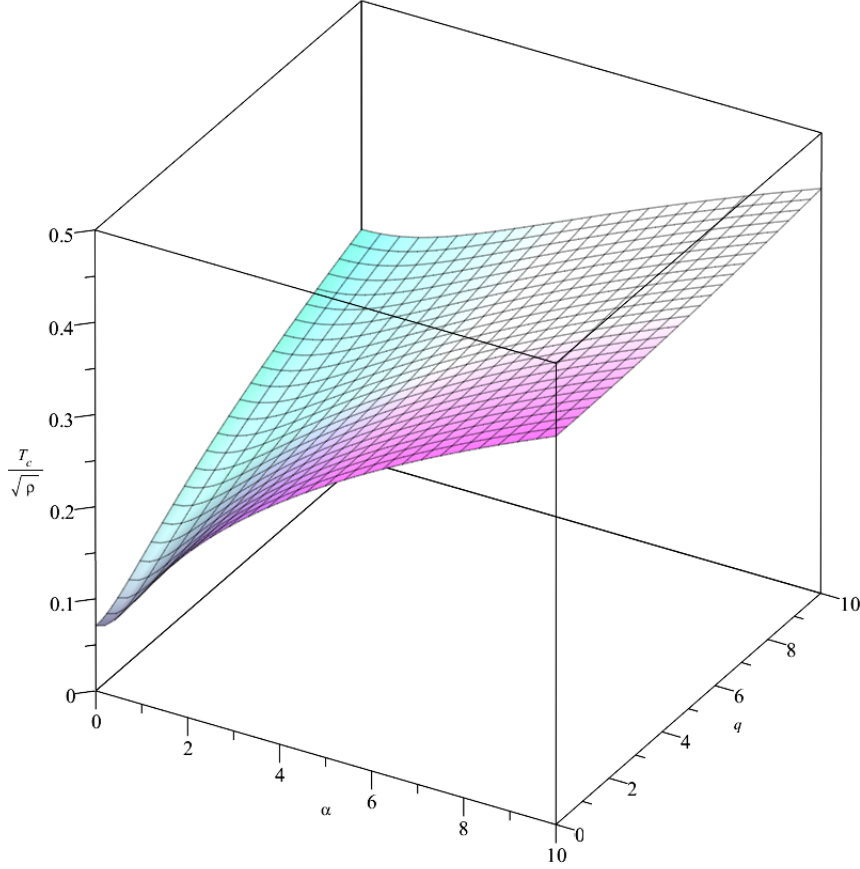


FIG. 6: The critical temperature T_c vary with the couplings α , q .

C. Conductivity

In this section, we compute the conductivity of this system by adding an external source A_x perturbatively. The metric is thus modified by a perturbative non-diagonal component g_{tx} . Defining $A_x = \tilde{A}_x(r) e^{-i\omega t}$ and $g_{tx} = \tilde{g}_{tx}(r) e^{-i\omega t}$, the equations of motion for the perturbative field $\tilde{A}_x(r)$ and $\tilde{g}_{tx}(r)$ are

$$\tilde{A}_x'' + \left(\frac{g'}{g} - \frac{\chi'}{2} + \frac{f'}{f} \right) \tilde{A}_x' + \left(\frac{\omega^2}{g^2} e^\chi - \frac{J}{gf} \right) \tilde{A}_x + \frac{A_t'}{g} e^\chi \left(\tilde{g}'_{tx} - \frac{2}{r} \tilde{g}_{tx} \right) = 0, \quad (4.6a)$$

$$\tilde{g}'_{tx} - \frac{2}{r} \tilde{g}_{tx} + f A_t' \tilde{A}_x = 0, \quad (4.6b)$$

which lead to a homogeneous linear differential equation for \tilde{A}_x ,

$$\tilde{A}_x'' + \left(\frac{g'}{g} - \frac{\chi'}{2} + \frac{f'}{f} \right) \tilde{A}_x' + \left[\left(\frac{\omega^2}{g^2} - \frac{f A_t'^2}{g} \right) e^\chi - \frac{J}{gf} \right] \tilde{A}_x = 0. \quad (4.7)$$

Making a coordinate transformation $z = r_H/r$ and defining $e^\chi \tilde{A}_x^2 = C^2$, the equation for \tilde{A}_x becomes

$$C''' + \left(\frac{g'}{g} - \frac{3}{2}\chi' + \frac{f'}{f} + \frac{2}{z} \right) C'' + \left[-\frac{1}{2}\chi'' + \frac{1}{2}\chi'^2 - \frac{1}{2}\chi' \left(\frac{g'}{g} + \frac{f'}{f} + \frac{2}{z} \right) + \left(\frac{r_H^2 \omega^2 e^\chi}{z^4 g^2} - \frac{f}{g} \left(B' - \frac{1}{2}\chi' B \right)^2 - \frac{r_H^2 J}{z^4 g f} \right) \right] C = 0. \quad (4.8)$$

To realize the structure of the Eq. (4.8), we make a further coordinate transformation,

$$du = -\frac{r_H e^{\frac{\chi}{2}}}{g z^2} dz, \quad (4.9)$$

which transforms the horizon at $z = 1$ to $u = -\infty$ and the boundary at $z = 0$ to $u = 0$.

We integrate the coordinate transformation (4.9) term by term to get

$$u = -\int \left(\frac{p_0}{1-z} + p_1 + \dots \right) dz = p_0 \ln(1-z) + p_1(1-z) + \dots, \quad (4.10)$$

where p_i 's are the expansion coefficients near the horizon at $z = 1$.

By defining a new field $\Psi = \sqrt{f} e^{-\chi/2} C$, the Eq.(4.8) can be brought to the form of the Schrodinger equation,

$$\frac{d^2 \Psi}{du^2} + [\omega^2 - V(u)] \Psi = 0, \quad (4.11)$$

where the potential is

$$V(u) = g \left[f \left(\frac{d(e^{-\chi/2} B)}{du} \right)^2 + \frac{J}{f} e^{-\chi} \right] + \frac{1}{\sqrt{f}} \frac{d^2 \sqrt{f}}{du^2}, \quad (4.12)$$

with $V(0) = V(-\infty) = 0$.

The Schrodinger equation (4.11) with the potential (4.12) is a standard one-dimensional scattering problem, and the wave function $\Psi(u)$ near the boundary at $u \sim 0$ behaves as

$$\Psi(u) = e^{-i\omega u} + R e^{i\omega u}, \quad (4.13)$$

where R is the reflection coefficient. The conductivity can thus be written as

$$\sigma(\omega) = \frac{1-R}{1+R}. \quad (4.14)$$

At the horizon at $u = -\infty$, the in-falling wave boundary condition admits a non-reflection wave function ,

$$\Psi(u) = T e^{-i\omega u}. \quad (4.15)$$

where T is the transmission coefficient.

In the z coordinate, the in-falling wave function becomes

$$\Psi = T e^{-i\omega[p_0 \ln(1-z) + p_1(1-z) + \dots]}. \quad (4.16)$$

Therefore, near the horizon, the field $C(z)$ can be expanded as,

$$\begin{aligned} C(z) &= c_0 e^{-i\omega[p_0 \ln(1-z) + p_1(1-z) + \dots]} \cdot [1 + c_1(1-z) + \dots] \\ &\simeq c_0 e^{-i\omega[p_0 \ln(1-z) + P_1(1-z)]} \cdot [1 + C_1(1-z)], \end{aligned} \quad (4.17)$$

where in the second line we assumed a truncated form of the field $C(z)$ with P_1 and C_1 being the effective coefficients by truncating all the higher-order terms at the horizon. Therefore, P_1 and C_1 contain the effects far from the horizon and will be determined by Eq. (4.17) and the boundary condition at $z = 0$. The approximated truncating solution is of course different from the true solution, but we will see that some important properties are preserved in this approximation.

At the boundary, the asymptotic form of $C(z)$ is

$$C(z) = C^{(0)} + \frac{C^{(1)}}{r_H} z + \dots. \quad (4.18)$$

Expanding the field $C(z)$ in Eq. (4.17) at the boundary $z = 0$, the conductivity can be calculated as follows [9],

$$\sigma(\omega) = \frac{1}{i\omega} \frac{C^{(1)}}{C^{(0)}} = r_H(p_0 + P_1) - \frac{r_H}{i\omega} \left(\frac{C_1}{1 + C_1} \right). \quad (4.19)$$

In the high frequency limit $\omega \rightarrow \infty$, the conductivity should approach to one due to the asymptotic AdS geometry, the above expression gives

$$P_1 = -p_0 + \frac{1}{r_H}. \quad (4.20)$$

The coefficients p_0 and C_1 can be now calculated by plugging the the field $C(z)$ in Eq. (4.17) into the equation of motion (4.8). The exact expressions of p_0 and C_1 are listed in the Appendix as Eqs. (B.3a) and (B.3b)..

The DC conductivity can be obtained from the low frequency expansion of the conductivity (4.19),

$$\sigma(\omega) = \Re(\sigma) + i\Im(\sigma), \quad (4.21)$$

$$\Re(\sigma) = \sigma_0 + O(\omega^2), \quad (4.22)$$

$$\Im(\sigma) = \sigma_{-1}\omega^{-1} + O(\omega). \quad (4.23)$$

where both σ_0 and σ_{-1} are real and they are given in Eq. (B.7) in the Appendix. At $\omega = 0$, the imaginary part of the conductivity $\Im(\sigma)$ is proportional to ω^{-1} . By Kramers-Kronig relations, this implies that the real part of the conductivity $\Re(\sigma)$ behaves as a delta function at $\omega = 0$, i.e. DC superconductivity.

In the high frequency, the conductivity can be expanded as,

$$\sigma(\omega) = 1 + \frac{i r_H}{\omega} + O(\omega^{-2}), \quad (4.24)$$

which gives $\sigma(\omega) \rightarrow 1$ as $\omega \rightarrow \infty$ that has been fixed by the choice of P_1 in Eq. (4.20).

The real and imaginary parts of the conductivity vs. frequency are plotted in Fig. 7 - 9.

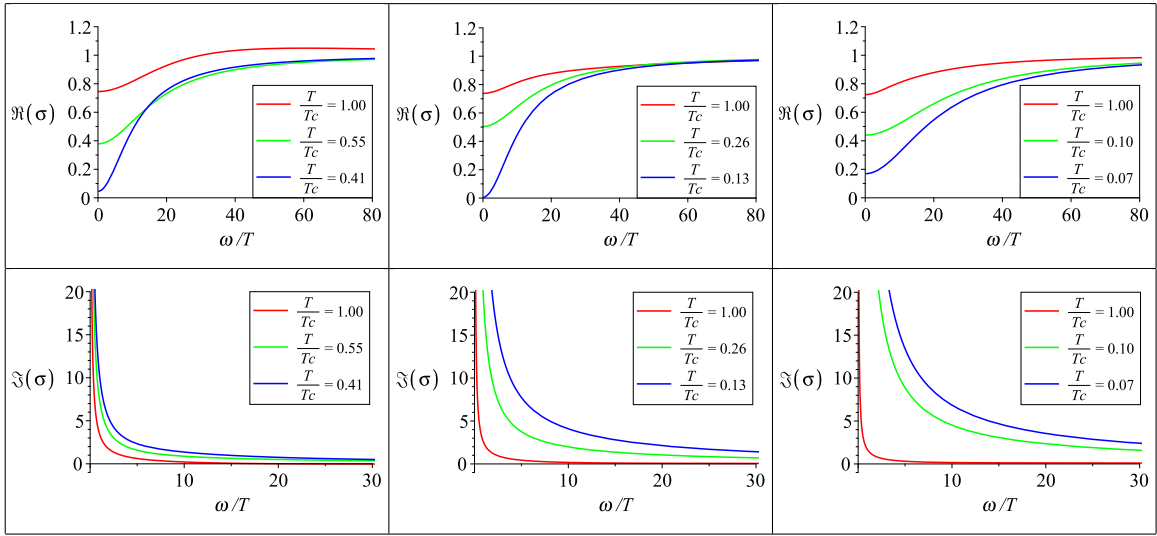


FIG. 7: The real and imaginary part of the conductivity with $\alpha = 1$ and $q = 1, 3, 5$ from left to right. The different curves in each figure are respect to different temperature ratio.

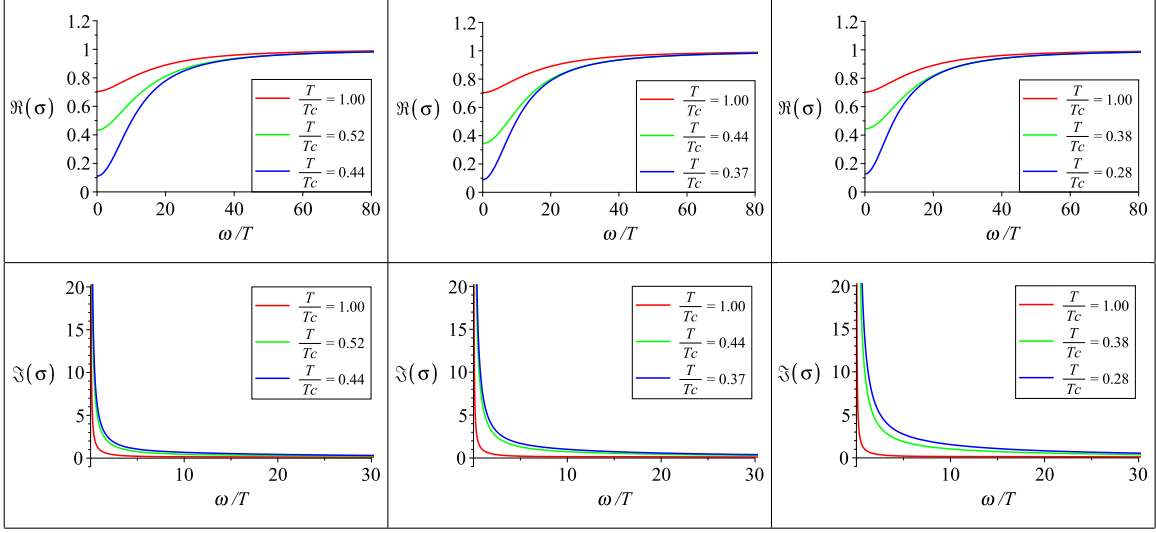


FIG. 8: The real and imaginary part of the conductivity with $\alpha = 3$ and $q = 1, 3, 5$ from left to right. The different curves in each figure are respect to different temperature ratio.

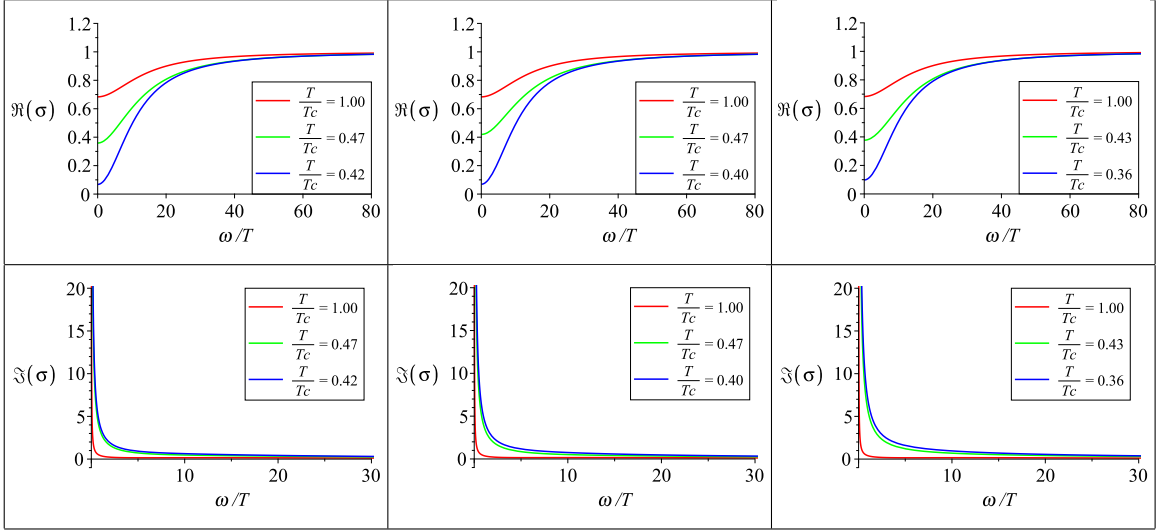


FIG. 9: The real and imaginary part of the conductivity with $\alpha = 5$ and $q = 1, 3, 5$ from left to right. The different curves in each figure are respect to different temperature ratio.

V. CONCLUSION

In this paper, we studied a non-minimal holographic superconductor model by considering the Einstein-Maxwell-Dilaton system. The model has two adjustable parameters α and q . α describes the coupling between the Maxwell field and the dilaton, and q represents the charge of the dilaton.

For various α and q , we solved the system analytically by an approximate method, the matching method. In this method, we only solved the equations of motion near the boundary and horizon, then matched the two asymptotic solutions smoothly at an intermediate matching point z_m between the boundary and the horizon. The matching solution ignores much details in the bulk, but surprisingly possesses many important properties which are consistent with the numeric results.

We studied both non-backreaction and the full-backreaction cases. We found phase transitions with the similar critical temperature T_c in both cases. The critical temperature increases with α and q monotonously and behaves as $T_c \propto \alpha^{1/2}$ for small q and $T_c \propto q^{1/2}$ for small α , which is consistent with the numeric results. The condensate near the critical temperature behaves as $(1 - T/T_c)^{1/2}$ which indicates that the phase transition is second order.

In the non-backreaction case, the behavior of the condensate at low temperature blows up quickly and is not make sense. Nevertheless, we showed that in the full-backreaction case, the low temperature behavior of the condensate is rectified. For a fixed α , the condensate increases as the parameter q increases, while for a fixed q , the condensate decreases as the parameter α increases. The behavior of the condensate depending on the parameters α and q is consistent with the numeric result.

In addition, we developed an approximate analytic method to calculate the electric conductivity. We expand the perturbative field A_x near the horizon obliged on the in-falling boundary condition of the Schrodinger equation at the horizon. We then truncated the expansion to the linear order and determined the truncating coefficients by the equation of motion and the boundary condition at the boundary. We showed that the imaginary part of the conductivity suffers a $1/\omega$ divergence at small frequency that implies the Dirac δ function behavior in the real part of the conductivity, i.e. DC superconductor. Furthermore, we showed that the asymptotic values of the real conductivity in the small frequency

limit increases as the temperature raised. However, we did not observe the "Drude Peak" behavior at the low frequency as in the numeric calculation [48].

In summary, we studied the condensation and electric conductivity a holographic superconductor model by using approximate analytic methods. The approximate solutions ignore some details of the system, but preserve many important physical properties. Since the analytic solutions are much more useful to investigate the critical phenomena than the numeric ones, it is worth to study various holographic models by using these analytic methods in the future.

Acknowledgements

We thank Chiang-Mei Chen, Mei Huang, Ming-Fan Wu and Pei-Hung Yuan for useful discussion. This work is supported by the Ministry of Science and Technology (MOST 106-2112-M-009-005-MY3) and in part by National Center for Theoretical Science (NCTS), Taiwan.

Appendices

A. CONDENSATE NEAR CRITICAL TEMPERATURE

Expanding the condensate around the critical temperature T_c , we obtain the approximate condensate for $T \leq T_c$,

$$D_2 = AT_c^2 \left(-\frac{T - T_c}{T_c} \right)^{1/2}, \quad (\text{A.1a})$$

$$A = \frac{11264\pi^4 T_c^4 - 81\alpha^2 \rho^2}{5184\pi^2 T_c^4} \left(-\frac{T_c}{T_1} \right)^{1/2}, \quad (\text{A.1b})$$

$$T = T_c + T_1 b^2 + O(b^4), \quad (\text{A.1c})$$

$$T_1 = \frac{\pi^4 \left(-2125824\pi^4 T_c^4 \alpha^2 - 77824\pi^4 T_c^4 q^2 + 22356\alpha^4 \rho^2 + 5670\alpha^2 q^2 \rho^2 + 243q^4 \rho^2 \right) T_c^5}{1944\rho^2 \left(\pi^4 T_c^4 q^2 + 10\pi^4 T_c^4 \alpha^2 - \frac{81\alpha^4 \rho^2}{512} \right)}, \quad (\text{A.1d})$$

B. FORMULAS WITH FULL-BACKREACTION

The near horizon coefficients with full-backreaction are listed here. The coefficients for the condensate background, (4.1), are written as follows:

$$\chi_1 = \frac{-8 \left[16b^2 r_H^4 + 4a^2(2\alpha^2 b^2 + 1)r_H^2 + a^4 \alpha^4 b^2 \right]}{\left[-4(b^2 + 6)r_H^2 + a^2(\alpha^2 b^2 + 2) \right]^2}, \quad (\text{B.2a})$$

$$g_1 = \frac{4b^2 r_H^2 - a^2(\alpha^2 b^2 + 2)}{8r_H^2}, \quad (\text{B.2b})$$

$$B_2 = \frac{-6a}{(\alpha^2 b^2 + 2) \left[-4(b^2 + 6)r_H^2 + a^2(\alpha^2 b^2 + 2) \right]^2} \cdot \left\{ -16b^2 \left[\frac{1}{3}(\alpha^2 + q^2)b^2 + 2 \left(2\alpha^2 + q^2 - \frac{1}{3} \right) \right] r_H^4 + \frac{4}{3}a^2 \left[\alpha^2(2\alpha^2 + q^2)b^4 - (12\alpha^4 - 9\alpha^2 - 2q^2)b^2 + 2 \right] r_H^2 + a^4 \alpha^4 (\alpha^2 b^2 + 2)b^2 \right\}, \quad (\text{B.2c})$$

$$\phi_1 = \frac{4b(4r_H^2 + a^2\alpha^2)}{-4(b^2 + 6)r_H^2 + a^2(\alpha^2 b^2 + 2)}, \quad (\text{B.2d})$$

$$\phi_2 = \frac{-4b}{(\alpha^2 b^2 + 2) \left[-4(b^2 + 6)r_H^2 + a^2(\alpha^2 b^2 + 2) \right]^3} \left\{ -64(b^2 + 12)(\alpha^2 b^2 + 2)r_H^6 + 16a^2 \left[\alpha^4(b^4 + 12b^2 + 6)b^2 - \alpha^2 \left((3q^2 - 2)b^4 + (18q^2 - 37)b^2 - 60 \right) - 2q^2 b^2 - 12q^2 + 10 \right] r_H^4 - 8a^4 \left[\alpha^6(b^6 + \frac{7b^4}{2} + 9b^2) - \alpha^4 \left(\left(\frac{3q^2}{2} - 4 \right) b^4 - \frac{27b^2}{2} + 6 \right) - \left(4(q^2 - 1)b^2 - 21 \right) \alpha^2 - 2q^2 \right] r_H^2 + a^6 \alpha^2 (\alpha^2 b^2 + 2) \cdot \left((\alpha^2 b^2 + 2)^2 + 2\alpha^2(2\alpha^2 b^2 - 1) \right) \right\}. \quad (\text{B.2f})$$

The coefficients of the near horizon expansion of the perturbed field $C(z)$ are:

$$p_0 = \frac{e^{\frac{\chi_0}{2}}}{(g_1 + 3)r_H}, \quad (\text{B.3a})$$

$$C_1 = \frac{\Gamma}{\Delta}, \quad (\text{B.3b})$$

where,

$$\begin{aligned}
\Gamma = & -2\left(\alpha^2(\chi_1 - 2)b^2 + 2\alpha^2b\phi_1 + 2\chi_1 - 4\right)\omega^2e^{\chi_0} \\
& + 4(g_1 + 3)\left\{\left[2\alpha^2\left(-\omega^2p_0^2 - i\left(\frac{3}{8}\chi_1 + \frac{1}{4}\right)\omega p_0 + \frac{\chi_1}{8}\right)b^2 + i\alpha^2\omega p_0\phi_1(1 - i\omega p_0)b\right.\right. \\
& - 4\omega^2p_0^2 - i\left(\frac{3}{2}\chi_1 + 1\right)\omega p_0 + \frac{\chi_1}{2}\left. \right]g_1 + \left[-9\alpha^2\omega^2p_0^2 - i\left(\frac{9}{4}\chi_1 + 3\right)\alpha^2\omega p_0\right. \\
& + q^2 + \frac{3}{4}\alpha^2\chi_1\left. \right]b^2 + 3i\alpha^2\omega p_0\phi_1(1 - i\omega p_0)b + 18\left(\frac{1}{3} - i\omega p_0\right)\left(\frac{\chi_1}{4} - i\omega p_0\right)\left. \right]r_H^2 \\
& + i\omega(\alpha^2b^2 + 2)\left(\frac{1}{2} - i\omega p_0\right)(g_1 + 3)r_H + \frac{1}{4}a^2(\alpha^2b^2 + 2)^2\left. \right\}, \tag{B.4}
\end{aligned}$$

$$\Delta = 2(\alpha^2b^2 + 2)\left(e^{\chi_0}\omega^2 + r_H^2(g_1 + 3)^2(1 - i\omega p_0)^2\right). \tag{B.5}$$

The cubic equation of a^2 can be written as:

$$\begin{aligned}
0 = & -128(\alpha^2b^2 + 2) \cdot \left(b^6 + \frac{31b^4}{2} + 77b^2 + 114\right)r_H^6 + 96a^2\left[\alpha^4b^8 + \left(\frac{65\alpha^4}{6} + 4\alpha^2\right)b^6\right. \\
& + \left(32\alpha^4 + \left(q^2 + \frac{127}{3}\right)\alpha^2 + 4\right)b^4 + \left(28\alpha^4 + \left(6q^2 + \frac{335}{3}\right)\alpha^2 + \frac{2q^2}{3} + \frac{124}{3}\right)b^2 \\
& + 40\alpha^2 + 4q^2 + \frac{302}{3}\left. \right]r_H^4 - 24a^4\left[\alpha^6b^8 + \left(\frac{37\alpha^6}{6} + 6\alpha^4\right)b^6 + \left(\frac{23\alpha^6}{3} + (q^2 + 35)\alpha^4\right.\right. \\
& + 12\alpha^2\left. \right)b^4 - \left(6\alpha^6 - 31\alpha^4 - \left(\frac{8q^2}{3} + 66\right)\alpha^2 - 8\right)b^2 + 4\alpha^4 + 26\alpha^2 + \frac{4q^2}{3} + \frac{124}{3}\left. \right]r_H^2 \\
& \cdot 2a^6(\alpha^2b^2 + 2) \cdot \left[\alpha^6b^6 + 3\alpha^4\left(\frac{\alpha^2}{2} + 2\right)b^4 - 2\alpha^2(2\alpha^4 - 3\alpha^2 - 6)b^2 + 2\alpha^2(\alpha^2 + 3) + 8\right]. \tag{B.6}
\end{aligned}$$

The DC expansion of the conductivity is:

$$\sigma_{DC}(\omega) = i\sigma_{-1}\omega^{-1} + \sigma_0 + O(\omega), \tag{B.7}$$

$$\begin{aligned}
= & i\left(1 - \frac{2(\alpha^2b^2 + 2)(g_1 + 3)r_H^2}{\Xi}\right)r_H\omega^{-1} + \left(1 - \frac{4p_0(\alpha^2b^2 + 2)(g_1 + 3)r_H^3}{\Xi} + \frac{\Phi}{\Xi^2}\right) \\
& + O(\omega), \tag{B.8}
\end{aligned}$$

where,

$$\Xi = \left[\left(\alpha^2 + \frac{4q^2}{(\chi_1 + 2)(g_1 + 3)} \right) b^2 + 2 \right] (\chi_1 + 2) (g_1 + 3) r_H^2 + a^2 (\alpha^2 b^2 + 2)^2, \quad (\text{B.9})$$

$$\Phi = 6 \left\{ p_0 \left[\left((\chi_1 + 2) g_1 + 3\chi_1 + 8 \right) b - \frac{4}{3} \phi_1 (g_1 + 3) \right] b \alpha^2 + (2\chi_1 + 4) g_1 + 6\chi_1 + 16 \right] r_H - \frac{2}{3} (\alpha^2 b^2 + 2) (g_1 + 3) \right\} (\alpha^2 b^2 + 2) (g_1 + 3) r_H^4. \quad (\text{B.10})$$

-
- [1] J. Bardeen, L. N. Cooper, and J. R. Schrieffer. Theory of Superconductivity. *Physical Review*, 108:1175–1204, December 1957.
- [2] J. Maldacena. The Large-N Limit of Superconformal Field Theories and Supergravity. *International Journal of Theoretical Physics*, 38:1113–1133, 1999.
- [3] S. S. Gubser, I. R. Klebanov, and A. M. Polyakov. Gauge theory correlators from non-critical string theory. *Physics Letters B*, 428:105–114, May 1998.
- [4] E. Witten. Anti-de Sitter space and holography. *Advances in Theoretical and Mathematical Physics*, 2:253–291, 1998.
- [5] I. R. Klebanov and E. Witten. AdS/CFT correspondence and symmetry breaking. *Nuclear Physics B*, 556:89–114, September 1999.
- [6] O. Aharony, S. S. Gubser, J. Maldacena, H. Ooguri, and Y. Oz. Large N field theories, string theory and gravity. *physrep*, 323:183–386, January 2000.
- [7] S. S. Gubser. Breaking an Abelian gauge symmetry near a black hole horizon. *Phys. Rev. D*, 78(6):065034, September 2008.
- [8] S. A. Hartnoll, C. P. Herzog, and G. T. Horowitz. Building a Holographic Superconductor. *Physical Review Letters*, 101(3):031601, July 2008.
- [9] S. A. Hartnoll, C. P. Herzog, and G. T. Horowitz. Holographic superconductors. *Journal of High Energy Physics*, 12:015, December 2008.
- [10] C. P. Herzog. TOPICAL REVIEW: Lectures on holographic superfluidity and superconductivity. *Journal of Physics A Mathematical General*, 42:343001, August 2009.
- [11] S. Franco, A. García-García, and D. Rodríguez-Gómez. A general class of holographic superconductors. *Journal of High Energy Physics*, 4:92, April 2010.

- [12] F. Aprile and J. G. Russo. Models of holographic superconductivity. *Phys. Rev. D* , 81(2):026009, January 2010.
- [13] G. T. Horowitz. Introduction to Holographic Superconductors. In E. Papantonopoulos, editor, *Lecture Notes in Physics, Berlin Springer Verlag*, volume 828 of *Lecture Notes in Physics, Berlin Springer Verlag*, pages 313–347, 2011.
- [14] G. T. Horowitz and M. M. Roberts. Holographic superconductors with various condensates. *Phys. Rev. D* , 78(12):126008, December 2008.
- [15] M. Montull, A. Pomarol, and P. J. Silva. Holographic Superconductor Vortices. *Physical Review Letters*, 103(9):091601, August 2009.
- [16] C. P. Herzog. Analytic holographic superconductor. *Phys. Rev. D* , 81(12):126009, June 2010.
- [17] G. T. Horowitz, J. E. Santos, and B. Way. Holographic Josephson Junctions. *Physical Review Letters*, 106(22):221601, June 2011.
- [18] A. Salvio. Holographic superfluids and superconductors in dilaton-gravity. *Journal of High Energy Physics*, 9:134, September 2012.
- [19] H. B. Zeng, Y. Tian, Z. Y. Fan, and C.-M. Chen. Nonlinear transport in a two dimensional holographic superconductor. *Phys. Rev. D* , 93(12):121901, June 2016.
- [20] L. Yin, H.-c. Ren, T. K. Lee, and D. Hou. Momentum analyticity of transverse polarization tensor in the normal phase of a holographic superconductor. *Journal of High Energy Physics*, 8:116, August 2016.
- [21] T.-S. Huang and W.-Y. Wen. Holographic Model of Dual Superconductor for Quark Confinement. *ArXiv e-prints*, July 2016.
- [22] K.-Y. Kim and C. Niu. Homes’ law in Holographic Superconductor with Q-lattices. *ArXiv e-prints*, August 2016.
- [23] A. Sheykhi, F. Shamsi, and S. Davatolhagh. The upper critical magnetic field of holographic superconductor with conformally invariant Power-Maxwell electrodynamics. *Canadian Journal of Physics*, 95:450–456, May 2017.
- [24] B. Pourhassan and M. M. Bagheri-Mohagheghi. Holographic superconductor in a deformed four-dimensional STU model. *European Physical Journal C*, 77:759, November 2017.
- [25] Y. Ling, P. Liu, and J.-P. Wu. Note on the butterfly effect in holographic superconductor models. *Physics Letters B*, 768:288–291, May 2017.
- [26] G. Alkac, S. Chakraborty, and P. Chaturvedi. Holographic P -wave superconductors in 1 +1

- dimensions. *Phys. Rev. D* , 96(8):086001, October 2017.
- [27] H. B. Zeng, Y. Tian, Z. Fan, and C.-M. Chen. Nonlinear conductivity of a holographic superconductor under constant electric field. *Phys. Rev. D* , 95(4):046014, February 2017.
- [28] O. DeWolfe, O. Henriksson, and C. Wu. A holographic model for pseudogap in BCS-BEC crossover (I): Pairing fluctuations, double-trace deformation and dynamics of bulk bosonic fluid. *Annals of Physics*, 387:75–120, December 2017.
- [29] Y.-F. Cai, S. Lin, J. Liu, and J.-R. Sun. Holographic Preheating: Quasi-Normal Modes and Holographic Renormalization. *ArXiv e-prints*, December 2016.
- [30] J. Erdmenger, M. Flory, M.-N. Newrzella, M. Strydom, and J. M. S. Wu. Quantum quenches in a holographic Kondo model. *Journal of High Energy Physics*, 4:45, April 2017.
- [31] S. A. Hartnoll, A. Lucas, and S. Sachdev. Holographic quantum matter. *ArXiv e-prints*, December 2016.
- [32] M. Natsuume and T. Okamura. Kibble-Zurek scaling in holography. *Phys. Rev. D* , 95(10):106009, May 2017.
- [33] A. Gorsky, E. Gubankova, R. Meyer, and A. Zayakin. S -duality for holographic p -wave superconductors. *Phys. Rev. D* , 96(10):106010, November 2017.
- [34] Z.-H. Li, Y.-C. Fu, and Z.-Y. Nie. Competing s-wave orders from Einstein-Gauss-Bonnet gravity. *Physics Letters B*, 776:115–123, January 2018.
- [35] A. Gorsky and F. Popov. On magnetic and vortical susceptibilities of the Cooper condensate. *Physics Letters B*, 774:135–138, November 2017.
- [36] A. Kundu. Flavours and infra-red instability in holography. *Journal of High Energy Physics*, 11:101, November 2017.
- [37] J.-P. Wu and P. Liu. Holographic superconductivity from higher derivative theory. *Physics Letters B*, 774:527–532, November 2017.
- [38] M. Kord Zangeneh, S. S. Hashemi, A. Dehyadegari, A. Sheykhi, and B. Wang. Optical properties of Born-Infeld-dilaton-Lifshitz holographic superconductors. *ArXiv e-prints*, October 2017.
- [39] A. Sheykhi, A. Ghazanfari, and A. Dehyadegari. Holographic conductivity of holographic superconductors with higher-order corrections. *European Physical Journal C*, 78:159, February 2018.
- [40] D. Parai, D. Ghorai, and S. Gangopadhyay. Noncommutative effects of charged black hole on

- holographic superconductors. *ArXiv e-prints*, January 2018.
- [41] S. I. Kruglov. Holographic superconductor with nonlinear arcsin-electrodynamics. *ArXiv e-prints*, January 2018.
- [42] A. Sheykhi, D. Hashemi Asl, and A. Dehyadegari. Conductivity of higher dimensional holographic superconductors with nonlinear electrodynamics. *Physics Letters B*, 781:139–154, June 2018.
- [43] D. Wen, H. Yu, Q. Pan, K. Lin, and W.-L. Qian. A Maxwell-vector p-wave holographic superconductor in a particular background AdS black hole metric. *Nuclear Physics B*, 930:255–269, May 2018.
- [44] J. Cheng, Q. Pan, H. Yu, and J. Jing. Refractive index in generalized superconductors with Born-Infeld electrodynamics. *European Physical Journal C*, 78:239, March 2018.
- [45] T. Ishii and K. Murata. Floquet superconductor in holography. *ArXiv e-prints*, April 2018.
- [46] G. T. Horowitz and M. M. Roberts. Zero temperature limit of holographic superconductors. *Journal of High Energy Physics*, 11:015, November 2009.
- [47] M. Cadoni, G. D’Appollonio, and P. Pani. Phase transitions between Reissner-Nordstrom and dilatonic black holes in 4D AdS spacetime. *Journal of High Energy Physics*, 3:100, March 2010.
- [48] Y. Liu and Y.-W. Sun. Holographic superconductors from Einstein-Maxwell-Dilaton gravity. *Journal of High Energy Physics*, 7:99, July 2010.
- [49] P. Basu, J. He, A. Mukherjee, M. Rozali, and H.-H. Shieh. Competing holographic orders. *Journal of High Energy Physics*, 10:92, October 2010.
- [50] W.-Y. Wen, M.-S. Wu, and S.-Y. Wu. Holographic model of a two-band superconductor. *Phys. Rev. D*, 89(6):066005, March 2014.
- [51] Y. Peng and Y. Liu. A general holographic metal/superconductor phase transition model. *Journal of High Energy Physics*, 2:82, February 2015.
- [52] A. Sheykhi and F. Shaker. Analytical study of holographic superconductor in Born-Infeld electrodynamics with backreaction. *Physics Letters B*, 754:281–287, March 2016.
- [53] A. Sheykhi and F. Shaker. Effects of backreaction and exponential nonlinear electrodynamics on the holographic superconductors. *International Journal of Modern Physics D*, 26:1750050, 2017.
- [54] Y. Peng and G. Liu. Holographic entanglement entropy in two-order insulator/superconductor

- transitions. *Physics Letters B*, 767:330–335, April 2017.
- [55] H. R. Salahi, A. Sheykhi, and A. Montakhab. Effects of backreaction on power-Maxwell holographic superconductors in Gauss-Bonnet gravity. *European Physical Journal C*, 76:575, October 2016.
- [56] M. Kord Zangeneh, Y. C. Ong, and B. Wang. Entanglement entropy and complexity for one-dimensional holographic superconductors. *Physics Letters B*, 771:235–241, August 2017.
- [57] Z. Sherkatghanad, B. Mirza, and F. Lalehgani Dezaki. Exponential nonlinear electrodynamics and backreaction effects on holographic superconductor in the Lifshitz black hole background. *International Journal of Modern Physics D*, 27:1750175, 2018.
- [58] D. Ghorai and S. Gangopadhyay. Conductivity of holographic superconductors in Born-Infeld electrodynamics. *ArXiv e-prints*, October 2017.
- [59] B. Binaei Ghotbabadi, M. Kord Zangeneh, and A. Sheykhi. One-dimensional backreacting holographic superconductors with exponential nonlinear electrodynamics. *ArXiv e-prints*, April 2018.
- [60] M. Mohammadi, A. Sheykhi, and M. Kord Zangeneh. Analytical and numerical study of backreacting one-dimensional holographic superconductors in the presence of Born-Infeld electrodynamics. *ArXiv e-prints*, May 2018.
- [61] N. Iqbal, H. Liu, M. Mezei, and Q. Si. Quantum phase transitions in holographic models of magnetism and superconductors. *Phys. Rev. D*, 82(4):045002, August 2010.
- [62] M. Rogatko and K. I. Wysokinski. Condensate flow in holographic models in the presence of dark matter. *Journal of High Energy Physics*, 10:152, October 2016.
- [63] Y. Peng. Studies of a general flat space/boson star transition model in a box through a language similar to holographic superconductors. *Journal of High Energy Physics*, 7:42, July 2017.
- [64] Y. Peng, B. Wang, and Y. Liu. On the thermodynamics of the black hole and hairy black hole transitions in the asymptotically flat spacetime with a box. *European Physical Journal C*, 78:176, March 2018.
- [65] T. Andrade, A. Krikun, K. Schalm, and J. Zaanen. Doping the holographic Mott insulator. *ArXiv e-prints*, October 2017.
- [66] Y. Peng. A general quasi-local flat space/boson star transition model and holography. *ArXiv e-prints*, October 2017.

- [67] Y. Ling, P. Liu, J.-P. Wu, and M.-H. Wu. Holographic superconductor on a novel insulator. *Chinese Physics C*, 42(1):013106, January 2018.
- [68] G. Filios, P. A. González, X.-M. Kuang, E. Papantonopoulos, and Y. Vásquez. Spontaneous Momentum Dissipation and Coexistence of Phases in Holographic Horndeski Theory. *arXiv e-prints*, August 2018.
- [69] O. Domènech, M. Montull, A. Pomarol, A. Salvio, and P. J. Silva. Emergent gauge fields in holographic superconductors. *Journal of High Energy Physics*, 8:33, August 2010.
- [70] M. Montull, O. Pujolàs, A. Salvio, and P. J. Silva. Flux Periodicities and Quantum Hair on Holographic Superconductors. *Physical Review Letters*, 107(18):181601, October 2011.
- [71] M. Montull, O. Pujolàs, A. Salvio, and P. J. Silva. Magnetic response in the holographic insulator/superconductor transition. *Journal of High Energy Physics*, 4:135, April 2012.
- [72] A. Salvio. Transitions in dilaton holography with global or local symmetries. *Journal of High Energy Physics*, 3:136, March 2013.
- [73] A. Dey, S. Mahapatra, and T. Sarkar. Generalized holographic superconductors with higher derivative couplings. *Journal of High Energy Physics*, 6:147, June 2014.
- [74] S. Mahapatra, P. Phukon, and T. Sarkar. Generalized superconductors and holographic optics. *Journal of High Energy Physics*, 1:135, January 2014.
- [75] S. Mahapatra. Generalized superconductors and holographic optics. Part II. *Journal of High Energy Physics*, 1:148, January 2015.
- [76] A. Amoretti, D. Areán, B. Goutéraux, and D. Musso. DC resistivity of quantum critical, charge density wave states from gauge-gravity duality. *ArXiv e-prints*, December 2017.
- [77] R. Gregory, S. Kanno, and J. Soda. Holographic superconductors with higher curvature corrections. *Journal of High Energy Physics*, 10:010, October 2009.
- [78] C. Chen and M. Wu. An Analytic Analysis of Phase Transitions in Holographic Superconductors. *Progress of Theoretical Physics*, 126:387–395, September 2011.
- [79] X. Ge and H. Leng. Analytical Calculation on Critical Magnetic Field in Holographic Superconductors with Backreaction. *Progress of Theoretical Physics*, 128:1211–1228, December 2012.
- [80] A. J. Nurbagambetov. Analytical approach to phase transitions in rotating and non-rotating 2D holographic superconductors. *ArXiv e-prints*, July 2011.
- [81] D. Roychowdhury. Effect of external magnetic field on holographic superconductors in pres-

- ence of nonlinear corrections. *Phys. Rev. D* , 86(10):106009, November 2012.
- [82] W.-H. Huang. Analytic Study of First-Order Phase Transition in Holographic Superconductor and Superfluid. *International Journal of Modern Physics A*, 28:1350140, October 2013.
- [83] A. Sheykhi and F. Shamsi. Holographic Superconductors with Logarithmic Nonlinear Electrodynamics in an External Magnetic Field. *International Journal of Theoretical Physics*, 56:916–930, March 2017.
- [84] Y. Ling and X. Zheng. Holographic superconductor with momentum relaxation and Weyl correction. *Nuclear Physics B*, 917:1–18, April 2017.
- [85] D. Ghorai and S. Gangopadhyay. Non-linear effects on the holographic free energy and thermodynamic geometry. *EPL (Europhysics Letters)*, 118:31001, May 2017.
- [86] S. R. Das, M. Fujita, and B. S. Kim. Holographic entanglement entropy of a 1 + 1 dimensional p-wave superconductor. *Journal of High Energy Physics*, 9:16, September 2017.
- [87] S. Pal and S. Gangopadhyay. Noncommutative effects on holographic superconductors with power Maxwell electrodynamics. *Annals of Physics*, 388:472–484, January 2018.